Journal of Theoretical Biology 291 (2011) 47–55

Contents lists available at SciVerse ScienceDirect

Journal of Theoretical Biology

journal homepage: www.elsevier.com/locate/yjtbi

Simulation of action potential propagation in plants

Vladimir Sukhov*, Vladimir Nerush, Lyubov Orlova, Vladimir Vodeneev

Department of Biophysics, N.I. Lobachevsky State University of Nizhny Novgorod, Nizhny Novgorod, Gagarin Avenue, 23, 603950, Russia

ARTICLE INFO

Article history:
Received 16 March 2011
Received in revised form
2 September 2011
Accepted 6 September 2011
Available online 21 September 2011

Keywords:
Action potential
Plants
Mathematical model
Cell to cell electrical conductivity
H^+-ATPase

ABSTRACT

Action potential is considered to be one of the primary responses of a plant to action of various environmental factors. Understanding plant action potential propagation mechanisms requires experimental investigation and simulation; however, a detailed mathematical model of plant electrical signal transmission is absent. Here, the mathematical model of action potential propagation in plants has been worked out. The model is a two-dimensional system of excitable cells; each of them is electrically coupled with four neighboring ones. Ion diffusion between excitable cell apoplast areas is also taken into account. The action potential generation in a single cell has been described on the basis of our previous model. The model simulates active and passive signal transmission well enough. It has been used to analyze theoretically the influence of cell to cell electrical conductivity and H^+-ATPase activity on the signal transmission in plants. An increase in cell to cell electrical conductivity has been shown to stimulate an increase in the length constant, the action potential propagation velocity and the temperature threshold, while the membrane potential threshold being weakly changed. The growth of H^+-ATPase activity has been found to induce the increase of temperature and membrane potential thresholds and the reduction of the length constant and the action potential propagation velocity.

1. Introduction

Action potential (AP) generation and propagation are considered to be one of the primary responses of a plant upon the actions of various environmental factors. AP induces a number of changes in physiological processes such as photosynthesis, respiration, phloem transport, gene expression and others (Fromm and Spanswick, 1993; Fromm and Bauer, 1994; Stankovic and Davies, 1996; Stankovic et al., 1998; Bulychev et al., 2004; Fromm and Lautner, 2007; Krupenina and Bulychev, 2007; Pyatygin et al., 2008; Grams et al., 2009). However, the way of electrical signal transformation into functional responses is still unclear. The understanding of AP generation and propagation mechanisms can facilitate the solution of this problem.

According to the current concept, the generation of AP is associated with passive fluxes of Ca^{2+}, Cl^- and K^+ (Fromm and Spanswick, 1993; Fromm and Bauer, 1994; Samejima and Sibaoka, 1982; Opritov and Retivin, 1982; Felle and Zimmermann, 2007). Reversible inactivation of the H^+-ATPase also possibly participates in the higher plant AP generation (Opritov et al., 2002; Vodeneev et al., 2006) like an electrical response in alga *Acetabularia* (Gradmann, 1976; Mummert and Gradmann, 1991).

Conducting vascular bundles are believed to be AP propagation pathways in plants (Fromm and Lautner, 2007; Sibaoka, 1991; Opritov et al., 1991; Dziubinska, 2003). There are two possible channels to transmit electrical signals: symplast of parenchyma cells (Sibaoka, 1962, 1991; Opritov et al., 1991) and sieve elements (Fromm and Lautner, 2007; Volkov, 2000). AP was registered in both types of cells (Fromm and Lautner, 2007; Sibaoka, 1991; Koziolek et al., 2003). Parenchyma cells and sieve elements are quite different electrophysiologically; in particular, they differ in cell to cell electrical conductivity (Fromm and Lautner, 2007; Dziubinska, 2003) and content of H^+-ATPase (Michelet and Boutry, 1996; Fleurat-Lessard et al., 1997), which is a basic primary active electrogenic ion transporter in the plasmalemma (Spanswick, 2006). The study of the influence of these two factors on the AP propagation may clear up the problem of electrical signal transmission in plants. The problem, however, is quite complicated for an experimental analysis methodologically (changes are to be required of the cell to cell conductivity and the H^+-ATPase activity over a lengthy stem part) as well as due to considerable lability of these parameters (Michelet and Boutry, 1996; Fleurat-Lessard et al., 1997; Holdaway-Clarke et al., 2000; Blackman and Overall, 2001). So, the application of theoretical approach here, in particular, the mathematical model approach, seems to be quite topical.

There are some models that consider the AP generation under external stimuli (Mummert and Gradmann, 1991; Beilby, 1982, 2007; Sukhov and Vodeneev, 2009) or deal with the electrical

* Corresponding author. Tel.: +7 8314656106; fax: +7 8314345056.
E-mail address: vssuh@mail.ru (V. Sukhov).

0022-5193/$ - see front matter © 2011 Elsevier Ltd. All rights reserved.
doi:10.1016/j.jtbi.2011.09.019

processes developing on plasmalemma without stimulation (Gradmann et al., 1993; Gradmann and Hoffstadt, 1998; Gradmann, 2001a,b; Tyerman et al., 2001; Shabala et al., 2006). However, there are only few works (Pietruszka et al., 1997; Garkusha et al., 2002; Sukhov et al., 2011), which describe theoretically the AP propagation in plants, but they do not take into account in detail an ion mechanism of the electrical response generation. Structure of the excitable cell symplast in plants is qualitative similar with the electrically coupled cardiomyocyte syncytium one in animals (Trebacz et al., 2006). This excitable structure can be described by of a two-dimensional system of excitable elements with local electrical connections (Beaumont et al., 1998; Wohlfart and Ohlen, 1999; Ten Tusscher and Panfilov, 2006; Ten Tusscher et al., 2006; Shajahan et al., 2009), which is a simplified model of the real three-dimensional tissue. Therefore, it can be used in the theoretical description of the AP propagation in the three-dimensional plant symplast (Garkusha et al., 2002; Sukhov et al., 2011).

The aim of this work is to develop a mathematical model of AP propagation in plants and to carry out a simulation analysis of the influence of the cell to cell electrical conductivity and plasmalemma H^+-ATPase activity on the electrical signal transmission in these objects.

2. The model

2.1. The action potential generation model

The AP generation has been simulated on the basis of our previous model (Sukhov and Vodeneev, 2005, 2009), with modifications. This model describes well the AP generation in higher plants as well as the ion fluxes during electrical response (Sukhov and Vodeneev, 2009) that allows to avoid a repeated model verification. Also, detailed description of the number of ion transport processes offers the challenge for the model using in analysis of interaction between cells, the electrical signals functional role, etc.

Fig. 1 shows the processes taken into account and basic equations. Passive ion transport systems (inward and outward K^+-channels, Cl^--channels and Ca^{2+}-channels) have been described by the Goldman–Hodgkin–Katz equation and the equations of the open state probability (p_o) dynamics. The systems of primary active ion transport (H^+-ATPase and Ca^{2+}-ATPase) have been simulated by the "two-state model" (Sukhov and Vodeneev, 2005, 2009; Hansen et al., 1981; Beilby and Shepherd, 2001), which takes into account two states of the pump: with an ion and without it. Velocity constants of transitions between these states depend on ion concentrations and membrane potential (Sukhov and Vodeneev, 2009). A secondary active transport (H^+/K^+ antiporter and $2H^+/Cl^-$ symporter) is described as a difference between fluxes directed to the apoplast and to the cytoplasm (Sukhov and Vodeneev, 2009).

The changes in ion concentrations in the cytoplasm and apoplast are described on the basis of flux equations taking into account the ratios between cell surface and volume and between apoplast and cell volumes (Sukhov and Vodeneev, 2005, 2009). Apoplastic (K^+ and H^+) and cytoplasmic (H^+) buffer capacities have also been simulated in the model (Sukhov and Vodeneev, 2005). An increase in the cytoplasmic Ca^{2+} concentration is known to induce Cl^- channel activation (Lewis et al., 1997; Berestovsky and Kataev, 2005) and H^+-ATPase inactivation (Vodeneev et al., 2006; Kinoshita et al., 1995). The dependences of their activities on calcium ions have been taken into account in the AP generation model (Sukhov and Vodeneev, 2009).

The temperature influence on primary and secondary systems of active transport is described by temperature coefficient $Q_{10}=3$ (Sukhov and Vodeneev, 2005, 2009).

The differential equation for E_m (Sukhov and Vodeneev, 2005, 2009) has been replaced in this work by the stationary one (Cotterill, 2002)

$$E_m = \frac{g_K E_K + g_{Cl} E_{Cl} + g_{Ca} E_{Ca} + g_{PH} E_{PH} + g_{PCa} E_{PCa} + g_{Sy} E_{Sy}}{g_K + g_{Cl} + g_{Ca} + g_{PH} + g_{PCa} + g_{Sy}} \quad (1)$$

where g_K, g_{Cl}, g_{Ca}, g_{PH}, g_{PCa} and g_{Sy} are electrical conductivities of K^+ channels, Cl^- channels, Ca^{2+}channels, H^+-ATPase, Ca^{2+}-ATPase

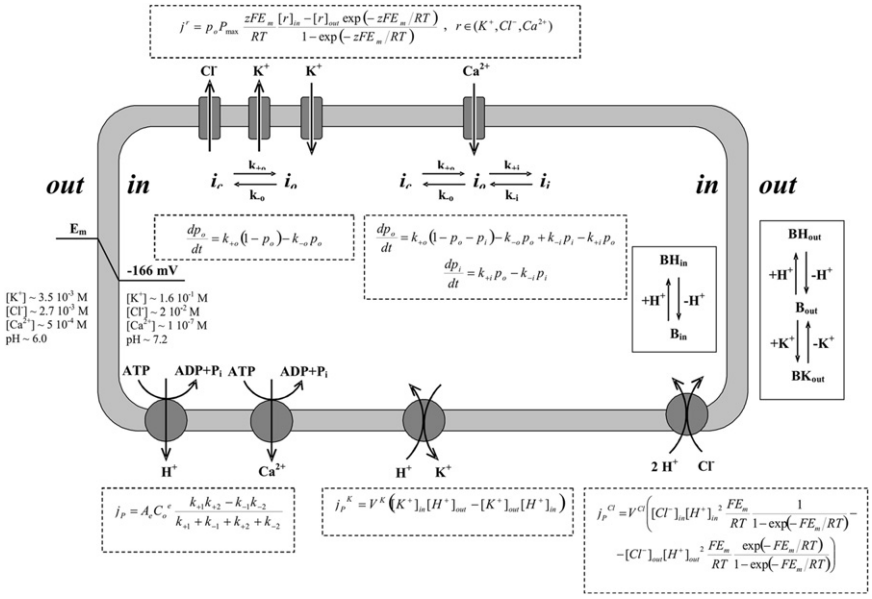

Fig. 1. Scheme of a plant cell electrophysiological model (Sukhov and Vodeneev, 2009, with modifications). E_m is the electrical potential of the plasma membrane; $[K^+]$, $[Cl^-]$ and $[Ca^{2+}]$ are the concentrations of potassium, chlorine and calcium ions, respectively (M); B_{in}^- and BH_{in} are free and H^+ bound proton-buffer molecules in the cell; B_{out}^-, BH_{out} and BK_{out} are free, H^+ and K^+-bound buffer molecules in the apoplast; P_{max} is the maximum permeability; p_o and p_i are the open state probability and the inactivated state probability of the ion channel; $k_{+o(+i)}$ and $k_{-o(-i)}$ are the velocity constants of ion channel transitions from the closed state to the open one and vice versa (subscript "*o*") or from the open state to the inactivated one and vice versa (subscript "*i*"); E_o is the ATPase concentration; k_{+1}, k_{-1}, k_{+2} and k_{-2} are velocity constants of forward (+) and reverse (−) transitions between two states of the pump; V^{Cl} and V^K are the total velocity constants of $2H^+/Cl^-$-symporter and H^+/K^+-antiporter, respectively.

and $2\,H^+/Cl^-$ symporter, respectively; $E_{PH}=(\Delta G_{ATP}/F)+E_H$, $E_{PCa}=(\Delta G_{ATP}/F)+E_{Ca}-E_H$ and $E_{Sy}=E_{Cl}+2E_H$ are equilibrium potentials of H^+-ATPase, Ca^{2+}-ATPase and $2\,H^+/Cl^-$ symporter fluxes, E_K, E_{Cl}, E_{Ca} and E_H are equilibrium potentials of K^+, Cl^-, Ca^{2+} and H^+. Eq. (2) has been used for the electrical conductivity:

$$g_k=-\frac{Fj_k}{E_m-E_k} \tag{2}$$

where j_k and E_k are the flux and the equilibrium potential for the process k, respectively.

Eq. (1) has been used because the AP development in the majority of higher plants is a slow process (from seconds to tens of seconds) (Sibaoka, 1991; Opritov et al., 1991; Trebacz et al., 2006), so the difference between the current membrane potential value and the stationary one is assumed to be very small for the conductivities used. Fig. 2 shows that cold-induced E_m changes do not depend on the type of description (differential or stationary). What is really important in the AP generation model with the stationary E_m is it can be numerically calculated (Euler's method) at $\Delta t=0.1$ s or more, whereas the model with the differential membrane potential requires $\Delta t\le 0.005$ s. This substantial increase in Δt simplifies the analysis of multi-cellular complexes used for the AP propagation simulation.

2.2. The action potential propagation model

A two-dimensional array of identical excitable cells (monolayer of ones) has been used to simulate the AP propagation (Fig. 3a). The length (L) of the array is 800 cells, and the width (W) is 30 cells. Each cell with its surrounding apoplast is considered as a single cubic element with dimensions $a\times a\times a=100\times 100\times 100\ \mu m^3$.

Each cell is electrically connected with four neighboring ones (Fig. 3b) in accordance with the symplast structure where neighboring cells are electrically connected via plasmodesmata (Fromm and Lautner, 2007; Sibaoka, 1991). Taking into account relatively small cell sizes and high intracellular conductivity it has been assumed that the AP propagation depends only on cell to cell conductivity in our model. Electrical currents depending on intercellular interactions are represented by

$$i_{lw}=\sum_{k,s} g_{lwks}(E_m{}^{ks}-E_m{}^{lw}) \tag{3}$$

where $l\in[1,L]$, $w\in[1,W]$, E_m^{lw} and E_m^{kr} are cell membrane potentials with positions $(l;w)$ and $(k;s)$, respectively, g_{lwkr} is the electrical conductivity between these cells and $(k;s)$ is equal to (l−1;w), (l+1;w), (l;w−1) or (l;w+1).

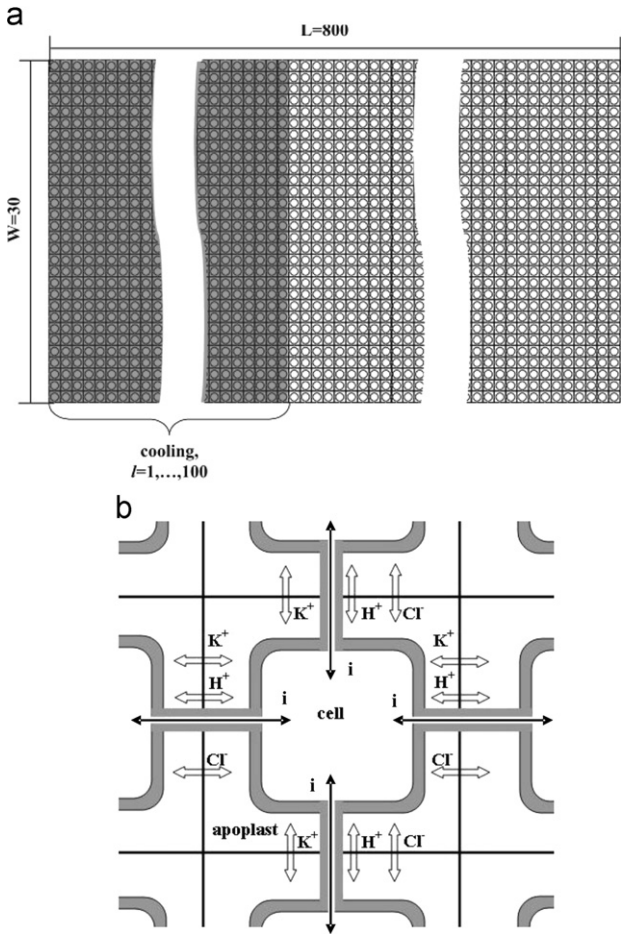

Fig. 3. Scheme of a two-dimensional array of identical excitable cells simulating the AP propagation (a), and its single cell fragment (b) i is cell to cell electric current.

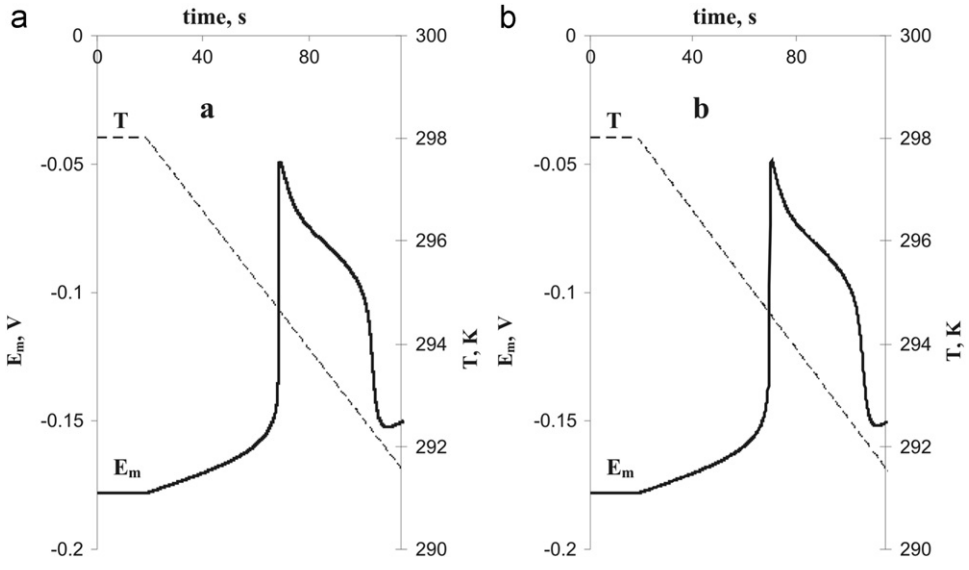

Fig. 2. Cold-induced membrane potential (E_m) changes simulated by differential (a) and stationary (b) descriptions E_m changes have been calculated by Euler's method at $\Delta t=5$ ms for the differential description and $\Delta t=100$ ms for the stationary one.

Using Eq. (1), we can find Eq. (4), which describes the stationary membrane potential for (l;w) cell:

$$E_m{}^{lw} = \frac{g_K E_K + g_{Cl} E_{Cl} + g_{Ca} E_{Ca} + g_{PH} E_{PH} + g_{PCa} E_{PCa} + g_{Sy} E_{Sy} + \sum_{k,s} g_{lwks} E_m{}^{ks}}{g_K + g_{Cl} + g_{Ca} + g_{PH} + g_{PCa} + g_{Sy} + \sum_{k,s} g_{lwks}} \quad (4)$$

where electrical conductivities of all plasmalemma ion transport systems and their equilibrium potentials relate to (l;w) cell. In this work $g_{lwks}=g$, where g is constant, i.e. cell to cell electrical conductivities are equal.

Diffusion changes of apoplastic ion concentrations (without Ca^{2+}) relating to (l;w) cell are described by Eq. (5) (Fig. 3), which is based on the Fick equation (Cotterill, 2002):

$$\frac{d[r]_{out}{}^{lw}}{dt} = \frac{D_r}{a^2(1+V_{cell}/V_{ap})} \sum_{k,s} ([r]_{out}^{ks} - [r]_{out}^{lw}) \quad (5)$$

where r is the type of ion, a is the array element dimension (100 μm), V_{cell}/V_{ap} is the ratio between apoplast and cell volumes, $D_K = 1.96 \times 10^{-5}$ cm s^{-1} (Samson et al., 2003), $D_{Cl} = 2.03 \times 10^{-5}$ cm s^{-1} (Samson et al., 2003) and $D_H = 7.8 \times 10^{-5}$ cm s^{-1} (Macpherson and Unwin 1997).

The above equations describing the AP propagation in plants are rather difficult to be applied for practical purposes due to considerable problems in their numerical solution: the propagation of E_m electronic changes, which plays a key role in AP transmission, is a very rapid process, because the plasmalemma time constant is equal to 0.1–2.0 ms in plants (Etherton, 1977; Ryser et al., 1999). As a result, $\Delta t \sim$tens μs is required for the adequate description of the AP propagation, which is becoming unrealistic for too long calculations.

This problem can be solved using the method described in work of Qu and Garfinkel (1999) with some modifications. Model equations have been calculated (Euler's method) using three values of Δt simultaneously: $\Delta t_1 = 100$ ms, a basic time step, has been used for the processes in the single cell without intercellular interactions, i.e. transmembrane fluxes, concentration changes, ion channel state transitions, etc.; $\Delta t_2 = 25$ μs has been used for the passive membrane potential change propagation (in Eq. (4) only membrane potentials are calculated every Δt_2, other values are calculated every Δt_1); $\Delta t_3 = 10$ ms has been used for ion diffusion between apoplast regions of neighboring cells (Eq. (5) has been calculated every Δt_3). These three values of Δt have been chosen as indicated since their further reduction is not essential for the calculation results.

2.3. Gradual cooling simulation

The AP generation is induced by the simulation of the gradual cooling used in a number of experimental works (Opritov et al., 1991, 2002, 2005; Vodeneev et al., 2006, 2007), as well as in our previous model (Sukhov and Vodeneev, 2009). First hundred lines of cells (Fig. 3, cells with $l \leq 100$) have been subjected to stimulation simulated as a linear decrease in the temperature (4 °C min^{-1}) from 25 to 10 °C. Cells with $l > 100$ have not been cooled.

2.4. Numerical solution of model equations

The model equations have been numerically calculated by Euler's method using the special computer program, which has been worked out with Borland Delphi 7. The values of model parameters have been described in previous work (Sukhov and Vodeneev, 2009). The values of the cell to cell electrical conductivity (g) and the plasma membrane H^+-ATPase activity ($A_e^{HATPase}$) have been varied. Variations of H^+-ATPase activity have been described as relative changes in enzyme concentration (C^e/C_0^e) where C_0^e is the concentration corresponding to $E_m = -180$ mV (see the AP generation model in work (Sukhov and Vodeneev, 2009)).

3. Results and discussion

3.1. Influence of cell to cell electrical conductivity and plasmalemma H^+-ATPase activity on the membrane potential without stimulation

At the first stage we have studied the influence of the cell to cell electrical conductivity and plasma membrane H^+-ATPase activity on the membrane potential without stimulation. In this case the changes in conductivity did not modify the membrane potential at rest (Fig. 4a), which is equal to −166 mV at $A_e^{H\text{-}ATPase} = 0.7$. This magnitude is in a good accordance with the membrane potential in plant cells usually ranging between −80 and −200 mV (Fromm and Lautner, 2007).

The dependence of the resting membrane potential on H^+-ATPase activity is shown in Fig. 4b ($g = 0.04$ S cm^{-2}). H^+-ATPase activity decrease has been accompanied with the resting potential reduction at $A_e^{H\text{-}ATPase}$ from 2 to 0.68 and from 0.25 to 0, while the stationary potential is not established at $A_e^{H\text{-}ATPase} \in 0.25; 0.68)$.

Fig. 4c shows the dynamics of the membrane potential at different H^+-ATPase activities (in (300,15) cell). Simulation of low activity ($A_e^{H\text{-}ATPase} = 0.1$) causes the spike and formation of the depolarized resting potential (−90 mV). Such changes of the membrane potential are in good agreement with its experimental dynamics at H^+-ATPase inhibition by external factors; in particular, the gradual cooling (Opritov et al., 1991; Pyatygin et al., 1999). Simulation of a moderate H^+-ATPase activity ($A_e^{H\text{-}ATPase} = 0.45$) disturbs the resting potential formation: the membrane potential depolarization, which is developed in this case, activates potential-dependent ionic channels and thereby induces oscillations of E_m (Fig. 4c). This result corresponds to experimental and theoretical studies (Gradmann, 2001a,b; Tyerman et al., 2001; Shabala et al., 2006; Thiel et al., 1992), which show the appearance and development of membrane potential and ionic flux oscillations in connection with H^+-ATPase activity. Simulation of a high H^+-ATPase activity ($A_e^{H\text{-}ATPase} = 1$) induces a monotonous formation of the high resting potential (−180 mV) (Fig. 4c), which is also in a good agreement with the membrane potential values in higher plant cells (Fromm and Lautner, 2007; Sibaoka, 1991; Opritov et al., 1991).

So, our model can describe the depolarized membrane potential, oscillations and the normal resting potential in plant cells. Transitions between different modes depend on H^+-ATPase activity, which correlates very well with experiments (Shabala et al., 2006; Pyatygin et al., 1999; Thiel et al., 1992). The cell to cell electrical conductivity does not affect the resting potential. Theoretical analysis of electrical signal propagation in plants is not possible to be carried out in the oscillatory mode; therefore we use H^+-ATPase activities more than 0.68 or less than 0.25 in what follows.

3.2. Simulation of the passive and active electrical signal propagation

The electrical signal propagation in plants can be active, which is connected with the AP generation in unstimulated cells, as well as passive, where membrane potential changes in unstimulated cells are electrotonic and the active electrical response is absent in these cells (Opritov and Retivin, 1982; Opritov et al., 1991). For the description of electrotonic membrane potential propagation, the calcium concentration has been decreased, as well as in work (Sukhov and Vodeneev, 2009), from $[Ca^{2+}]_{out} = 0.5$ mM to $[Ca^{2+}]_{out} = 0.5$ μM in the apoplast regions of unstimulated cells ($l > 100$), since the decrease of Ca^{2+}

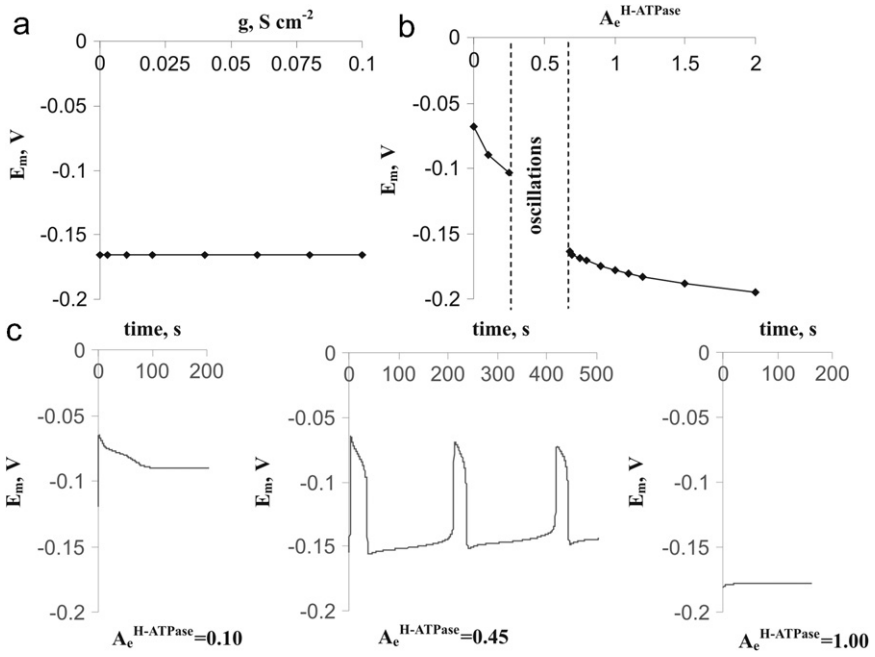

Fig. 4. Dependence of the membrane potential (E_m) at rest on the cell to cell electrical conductivity (g) (a) and H^+-ATPase activity ($A_e^{H\text{-}ATPase}$) (b) and examples of E_m dynamics in cell (300; 15) at different H^+-ATPase activities (c).

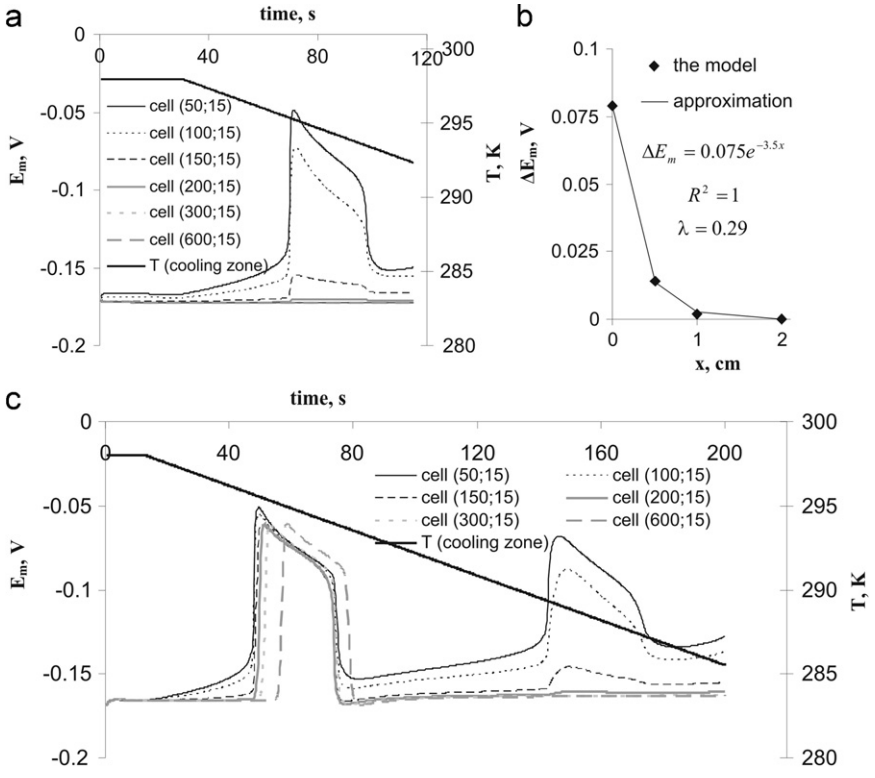

Fig. 5. Passive (a) and active (c) electrical signal propagation and a dependence (b) of the electrical response amplitude (ΔE_m) on a distance (x) from the stimulated region at the passive propagation. The cell to cell electrical conductivity (g) equals to 0.04 S cm^{-2}, the plasmalemma H^+-ATPase activity ($A_e^{H\text{-}ATPase}$) equals to 0.7; (l; 15) is the position of a cell, cells with $l \leq 100$ are stimulated, cell size equals to $100 \times 100 \times 100$ μm^3, λ is the length constant, solid line is an exponential trend.

suppresses the AP generation in higher plants in experiments (Felle and Zimmermann, 2007; Vodeneev et al., 2006; Iijima and Sibaoka, 1985; Hodick and Sievers, 1988). It should be noted that internal sources of Ca^{2+} can play some role in the AP generation (Biskup et al., 1999; Trewaves, 1999; Wacke and Thiel, 2001), but these mechanisms have not been taken into account here. Also, the model does not take into account Ca^{2+} influence on the whole plasma membrane (changes of membrane stability, fluidity, etc.) (Opritov et al., 1991), i.e. the external Ca^{2+} decrease is not stressor in our model. As a result, the external Ca^{2+} drop fully suppresses the active AP propagation in unstimulated cells in the model; at that calcium influence on the whole plasmalemma is not simulated.

Fig. 5 shows the passive and active electrical signal propagation (g=0.04 S cm^{-2} and $A_e^{H\text{-}ATPase}$=0.7) simulated by the model.

The simulation of the passive electrical signal propagation (Fig. 5a) shows that the response in stimulated cells (electrical reactions in cells (50; 15) and (100; 15) are shown) includes subthreshold changes of the membrane potential, the depolarization phase and the repolarization phase formed by two stages. This dynamics is consistent with experimental membrane potential changes in the cooling zone of plant (Opritov et al., 1991, 2002, 2005; Vodeneev et al., 2006, 2007; Pyatygin et al., 1999; Krol et al., 2003, 2004). However, as the distance from the stimulation zone increases, the amplitude of electrical responses decreases exponentially (electrical reactions in cells (150; 15), (200; 15), (300; 15) and (600; 15) are shown) that corresponds to the passive electrical reaction propagation in experiments (Opritov et al., 1991).

Fig. 5b shows the electrical response amplitude dependence on the distance from the stimulation zone simulated by the model, and the length constant calculation. In this variant, the length constant is equal to 0.29 cm, which is in a good agreement with the experimental magnitude in the range of 0.28–0.55 cm obtained for *Cucurbita pepo* L. Pyatygin (2008). Besides, the cell to cell electrical conductivity (0.04 S cm^{-2}) is close to the experimental one for *Elodea canadensis* (0.02 S cm^{-2}) (Spanswick, 1972). All these confirm the correctness of our description.

The simulation of the active electrical signal propagation (all cells are excitable) shows the workability of the model as well (Fig. 5c). In this case APs are generated in the unstimulated zone (electrical reactions are shown in cells (150; 15), (200; 15), (300; 15) and (600; 15)) as well as in the cold-stimulated zone (cells (50; 15) and (100; 15)); AP parameters in the unstimulated region are not dependent on the distance from the stimulation zone. The electrical signal propagation velocity is constant. This result is in a good qualitative agreement with experimental data on AP propagation in higher plants (Fromm and Lautner, 2007; Opritov et al., 1991; Trebacz et al., 2006; Davies, 2006).

The simulated AP propagation velocity is equal to 0.6 cm s^{-1}, which is in a good quantitative accordance with corresponding experimental values for most plants without motor activity: from several mm s^{-1} or less (Stankovic and Davies, 1996; Stankovic et al., 1998; Grams et al., 2009; Felle and Zimmermann, 2007; Dziubinska, 2003; Zawadzki et al., 1991, 1995; Volkov and Haack, 1995; Favre et al., 2001; Favre and Degli Agosti, 2007) to several cm s^{-1} (Fromm and Spanswick, 1993; Fromm and Bauer, 1994; Fromm et al., 1995; Grams et al., 2007). Moreover, the length constant 0.3 cm corresponds to the cold-induced AP velocity of 0.5 ± 0.2 cm s^{-1} in *Cucurbita pepo* L. (calculated on the basis of data in Pyatygin (2008)) that additionally supports the model correctness.

Magnitudes of other AP parameters also correlate with the experimental ones. The membrane potential threshold, calculated as the difference between resting E_m and E_m at the beginning of rapid depolarization (Opritov et al., 1991), are equal to 36 mV in the cold-stimulated zone center (cell (50; 15), the first spike); this lies in the range obtained in the experiment (from 30 to 70 mV (Pyatygin, 2008)). The membrane potential threshold in the unstimulated zone (cell (300; 15)) decreases up to 20 mV that correlates with 12–30 mV in the experiment (Pyatygin, 2008).

The total amplitude of the simulated electrical response (subthreshold E_m changes+AP) in stimulated cells is equal to 115 mV (cell (50; 15)) that corresponds to experimental amplitudes of electrical reactions induced by the gradual cooling in *Cucurbita pepo* L. (100–120 mV and more (Opritov et al., 1991, 2002, 2005; Pyatygin et al., 1999)). The simulated AP amplitude in the unstimulated zone (cell (300; 15)) is equal to 105 mV that lies in the AP amplitude range of most plants without motor activity (from 30–50 mV (Stankovic et al., 1998; Grams et al., 2009; Zawadzki et al., 1991) to 100 mV and more (Opritov et al., 1991; Wacke and Thiel 2001; Favre et al., 2001; Favre and Degli Agosti 2007; Fromm et al., 1995).

The simulated AP duration in stimulated (cell (50; 15)) and unstimulated (cell (300; 15)) zones is equal to 30 and 26 s, respectively; for most plants without motor activity, it ranges in the experiment from several seconds (Fromm et al., 1995) to tens of seconds and more (Opritov et al., 1991, 2002; Vodeneev et al., 2006, 2007; Krol et al., 2003, 2004; Favre and Degli Agosti, 2007).

It should be noted that the gradual cooling induces the series of repetitive APs in the stimulated zone; however, only the first spike propagates actively, while the second one is transmitted passively. This result also correlates well with the series of AP under gradual cooling in the experiment (Opritov et al., 1991, 2002, 2005; Pyatygin et al., 1999), together with the ability to propagate for only a single AP (Opritov et al., 1991, 2005).

Thus, simulated electrical responses in passive and active electrical signal propagation in plants are in a good qualitative and quantitative agreement with the experimental data that confirms the validity of our model. So, it can be used in the subsequent theoretical analysis of the influence of g and $A_e^{H\text{-}ATPase}$ on the AP propagation.

3.3. *Influence of cell to cell electrical conductivity and plasmalemma H^+-ATPase activity on the passive electrical signal propagation*

Fig. 6 shows the influence of cell to cell electrical conductivity and plasmalemma H^+-ATPase activity on the length constant (λ). The growth of g induces the nonlinear rise of λ (Fig. 6a). As it is known (Cotterill, 2002), λ can be calculated using (6) derived from the cable equation:

$$\lambda = \sqrt{\frac{G_{in}}{G_m}} \tag{6}$$

where G_m is the total plasmalemma conductivity per unit length, G_{in} is the total inner conductivity of the excitable structure per unit length depending on intracellular and cell to cell conductivities. In our model the intracellular resistance is not taken into account; so we have assumed that G_{in} depends only on g. G_m and G_{in} have been calculated by $G_m = 6g_mWa$ and $G_{in} = 4gWa^3$, where $W=30$ cells is the width of the system, $a=10^{-2}$ cm is the array

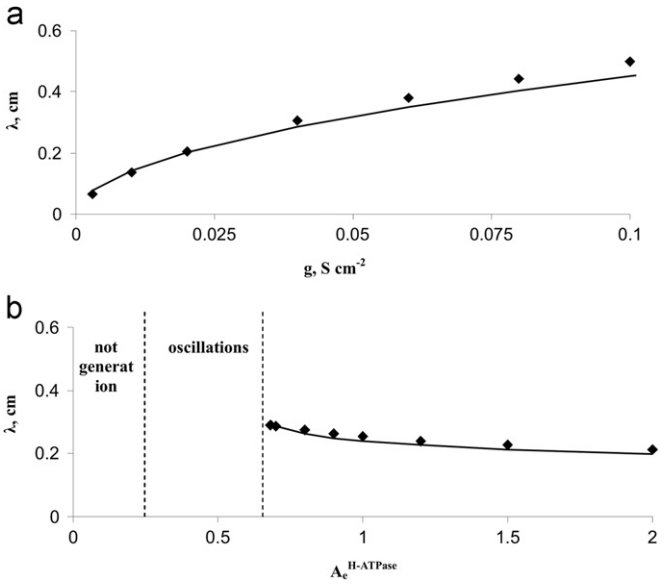

Fig. 6. Dependence of the length constant (λ) on the cell to cell electrical conductivity (a) and plasmalemma H^+-ATPase activity (b). Solid lines are trends (see the text).

element dimension, g_m is the total plasmalemma conductivity per unit area, "6" reflects six surfaces of cubic cells, which contain transporters of ions, and "4" corresponds with four ones, which contain plasmodesmata in our model (Fig. 3b). Therefore, Eq. (6) is transformed into

$$\lambda = \sqrt{\frac{4ga^2}{6g_m}} \quad (7)$$

It should be noted that g_m is not changed in this variant of analysis ($A_e^{H\text{-}ATPase}=0.7$, g is varied) and is equal to 3.2×10^{-5} S cm^{-2}. The last result is in agreement with data of literature (3×10^{-6}–8×10^{-5} S cm^{-2} in plants (Spanswick, 2006; Holdaway-Clarke et al., 2000; Beilby, 2007; Pyatygin, 2008)) and supports correctness of the model. Fig. 6a shows that Eq. (7) well describes dependence of λ on g at these conditions (trend line). Thus, it can be suggested that growth of g increases λ according to the cable equation.

The length constant dependence on the plasmalemma H^+-ATPase activity is shown in Fig. 6b. It should be noted that λ has only been calculated for $A_e^{H\text{-}ATPase} \geq 0.68$, since at low values (less than 0.25) the AP generation has been suppressed, which fits experimental data reasonably well (Vodeneev et al., 2006), and the moderate ones have induced membrane potential oscillations. When $A_e^{H\text{-}ATPase} \geq 0.68$, the growth of proton pump activity has caused a weak decrease of λ (from 0.29 to 0.21 cm).

It should be noted that the experimental confirmation of the plasmalemma H^+-ATPase activity influence on the length constant in higher plants is absent. However, this theoretical result can be well explained using the cable equation. In this case g does not change and equals to 0.04 S cm^{-2}, while g_m increases from 2.9×10^{-5} S cm^{-2} ($A_e^{H\text{-}ATPase}=0.68$) to 6.8×10^{-5} S cm^{-2} ($A_e^{H\text{-}ATPase}=2.00$) (data no shown). The H^+-ATPase conductivity rises from 0.6×10^{-5} S cm^{-2} ($A_e^{H\text{-}ATPase}=0.68$) to 2.3×10^{-5} S cm^{-2} ($A_e^{H\text{-}ATPase}=2.00$) (data no shown), that supports direct H^+-ATPase participation in growth of g_m. Fig. 6b shows that Eq. (7) well describes dependence of λ on $A_e^{H\text{-}ATPase}$ under different acivities of H^+-ATPase (trend line).

Thus, our theoretical analysis shows that the cell to cell electrical conductivity and the plasmalemma H+-ATPase activity can influence on the passive electrical signal propagation. In particular, the changes of these parameters may induce the length constant modifications. However, the parameters of the passive electrical signal transmission influence the AP propagation (Cotterill, 2002; Pyatygin, 2008); therefore, the simulated active electrical signal transmission also possibly depends on the electrical conductivity between cells and the plasmalemma H+-ATPase activity.

3.4. *Influence of cell to cell electrical conductivity and plasmalemma H^+-ATPase activity on the active electrical signal propagation*

Fig. 7 shows the influence of cell to cell electrical conductivity and plasmalemma H^+-ATPase activity on the simulated AP propagation velocity. The growth of electrical conductivity induces a nonlinear rise of AP velocity (Fig. 7a) from 0.17 cm s^{-1} (0.003 S cm^{-2}) to 0.8 cm s^{-1} (0.1 S cm^{-2}). This result is a good illustration of the connection between the AP propagation and the cell to cell electrical conductivity, in particular, the electrical conductivity of plasmodesmata (Sibaoka, 1991; Opritov et al., 1991; Dziubinska, 2003). It confirms our previous data (Sukhov et al., 2011), which showed that growth of conductivity between cells accelerated the AP propagation in a simple two-dimensional model on base of the FitzHugh–Nagumo equations. The increase in plasmalemma H^+-ATPase activity induces the reduction in AP propagation velocity, which has been simulated by the model

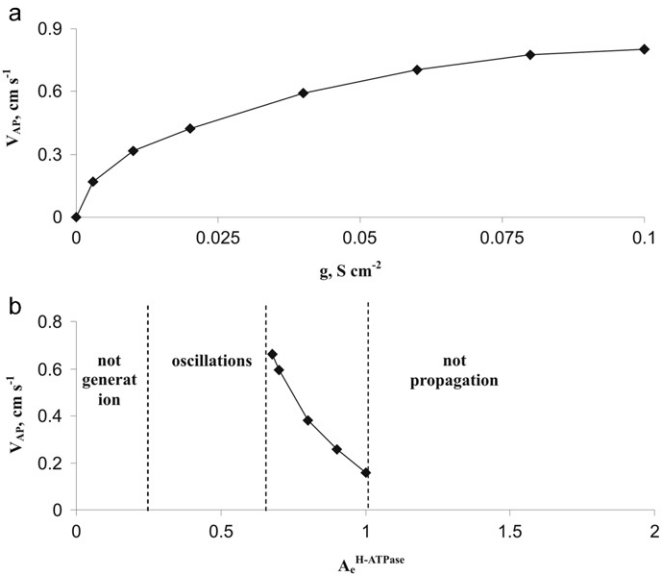

Fig. 7. Dependence of the AP propagation velocity (V_{AP}) on (a) the cell to cell electrical conductivity and (b) plasmalemma H^+-ATPase activity.

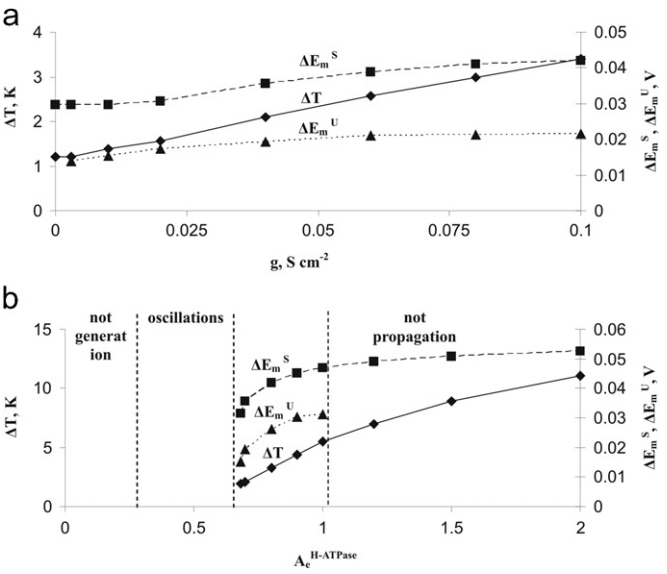

Fig. 8. Dependences of temperature and membrane potential thresholds on (a) the cell to cell electrical conductivity and (b) plasmalemma H^+-ATPase activity ΔT is the temperature threshold calculated as the difference between initial temperature and temperature at the beginning of rapid depolarization, ΔE_m^S is the membrane potential threshold in the stimulated cell (50; 15), ΔE_m^U is the membrane potential threshold in the unstimulated cell (600; 15). The membrane potential thresholds have been calculated as the difference between resting E_m and E_m at the beginning of rapid depolarization.

(Fig. 7b). It should be noted that the AP generation has not been observed at $A_e^{H\text{-}ATPase} < 0.68$ and the AP propagation has been suppressed at $A_e^{H\text{-}ATPase} > 1$.

Dependences of temperature and membrane potential thresholds on g and $A_e^{H\text{-}ATPase}$ are shown in Fig. 8. The temperature threshold has been calculated as the difference between initial temperature and temperature at the beginning of rapid depolarization. The membrane potential thresholds have been calculated as the difference between resting E_m and E_m at the beginning of rapid depolarization.

The increase in conductivity has induced an essential rise of the temperature threshold (from 1.2 to 3.5 K) simulated by the model, whereas membrane potential thresholds in the stimulated

(cell (50; 15)) and unstimulated (cell (600; 15)) zones are weakly changed (Fig. 8a). This influence is possibly connected with the increase in electrodiffusion and charge dissipation due to the growth of g. The growth of H^+-ATPase activity induces the rise of the temperature threshold as well as the membrane potential one (Fig. 8b). This process is possibly connected with the reduction of the resting membrane potential (Fig. 4a).

Taken together, these results theoretically show that growth of the cell to cell electrical conductivity accelerates AP propagation. It is rather connected with increase in the length constant, which strongly depends on g (Fig. 6a), than with change in the membrane potential threshold weakly depended on g (Fig. 8a). It should be noted that the temperature threshold (stimulated zone) essentially increases under growth of the cell to cell electrical conductivity, i.e. g rise hampers the AP generation. On the other hand, acceleration of the action potential propagation induced by decrease of the plasmalemma H^+-ATPase activity is rather connected with lowering of the membrane potential threshold, which strongly depends on $A_e^{H\text{-}ATPase}$ (Fig. 8b), whereas λ change is weak under these conditions (Fig. 6b). However, there is some minimal H^+-ATPase activity, which is necessary for generation and propagation of AP ($A_e^{H\text{-}ATPase}=0.68$).

Thus, our results show that optimal conductivity for the AP generation (the low temperature threshold) can differ from the optimal conductivity for the AP transmission (low velocity). The H^+-ATPase activity decrease can compensate this effect; but the low enzyme activity suppresses the AP generation.

4. Conclusion

The elaborated model of the AP propagation describes the basic features of the passive and active electrical signal transmission. The values of signal propagation parameters (the length constant, the AP velocity, electrical response amplitude and threshold) are in a good quantitative accordance with the experimental data. From all this it follows that the model can be used for the theoretical investigation of the AP propagation under different conditions.

The model has shown that the cell to cell electrical conductivity and the plasmalemma H^+-ATPase activity influence AP generation and propagation parameters. This influence can rather intricate that the conductivity rise induces simultaneously the growth of AP propagation velocity and the AP generation threshold; the H^+-ATPase activity rise can induce the AP propagation velocity reduction and the threshold growth, but a considerable drop in the activity ($A_e^{H\text{-}ATPase}<0.68$) disrupts the electrical response generation. These results provide a theoretical grounding for understanding that cell to cell electrical conductivity and the plasmalemma H^+-ATPase activity are essential factors influencing on AP generation and propagation. In particular, they show that sieve elements possessing the high electrical conductivity between cells (Fromm and Lautner, 2007) and the low plasma membrane H^+-ATPase content (Fleurat-Lessard et al., 1997) can be a good system of the AP transmission, but not optimal for the AP generation.

A further analysis of the AP propagation mechanisms requires the investigation of heterogeneous systems consisted of the elements with weak electrical coupling (parenchyma cells) and the elements with strong electrical coupling (sieve elements).

Acknowledgments

This work is supported by the Russian Foundation for Basic Research (Grant no. 09-04-01413-a).

References

Beaumont, J., Davidenko, N., Davidenko, J.M., Jalife, J., 1998. Spiral waves in two-dimensional models of ventricular muscle: formation of a stationary core. Biophys. J. 75, 1–14.
Beilby, M.J., 1982. $C1^-$ channels in *Chara*. Phil. Trans. R. Soc. Lond. B. 299, 435–445.
Beilby, M.J., 2007. Action potential in charophytes. Int. Rev. Cytol. 257, 43–82.
Beilby, M.J., Shepherd, V.A., 2001. Modeling the current-voltage characteristics of charophyte membranes. II. The effect of salinity on membranes of *Lamprothamnium papulosum*. J. Membrane Biol. 181, 77–89.
Berestovsky, G.N., Kataev, A.A., 2005. Voltage-gated calcium and Ca^{2+}-activated chloride channels and Ca^{2+} transients: voltage-clamp studies of perfused and intact cells of *Chara*. Eur. Biophys. J. 34, 973–986.
Biskup, B., Gradmann, D., Thiel, G., 1999. Calcium release from $InsP_3$-sensitive internal stores initiates action potential in *Chara*. FEBS Lett. 453, 72–76.
Blackman, L.M., Overall, R.L., 2001. Structure and function of plasmodesmata. Aust. J. Plant. Physiol. 28, 709–727.
Bulychev, A.A., Kamzolkina, N.A., Luengviriya, J., Rubin, A.B., Muller, S.C., 2004. Effect of a single excitation stimulus on photosynthetic activity and light-dependent pH banding in *Chara* cells. J. Membrane Biol. 202, 11–19.
Cotterill, R.M.J., 2002. Biophysics. An Introduction. John Wiley & Sons Ltd., Chichester.
Davies, E., 2006. Electrical signals in plants: facts and hypotheses. In: Volkov, A.G. (Ed.), Plant Electrophysiology. Theory and Methods, Springer, Berlin-Heidelberg, pp. 407–422.
Dziubinska, H., 2003. Ways of signal transmission and physiological role of electrical potential in plants. Acta Soc. Bot. Pol. 72, 309–318.
Etherton, B., 1977. Comparison of three methods for measuring electrical resistances of plant cell membranes. Plant Physiol. 60, 684–688.
Favre, P., Degli Agosti, R., 2007. Voltage-dependent action potentials in *Arabidopsis thaliana*. Physiol. Plant 131, 263–272.
Favre, P., Greppin, H., Degli Agosti, R., 2001. Repetitive action potentials induced in Arabidopsis thaliana leaves by wounding and potassium chloride application. Plant Physiol. Biochem. 39, 961–969.
Felle, H.H., Zimmermann, M.R., 2007. Systemic signaling in barley through action potentials. Planta 226, 203–214.
Fleurat-Lessard, P., Bouche-Pillon, S., Leloup, C., Bonnemain, J.-L., 1997. Distribution and activity of the plasma membrane H^+-ATPase in *Mimosa pudica* L. in relation to ionic fluxes and leaf movements. Plant Physiol. 113, 747–754.
Fromm, J., Bauer, T., 1994. Action potentials in maize sieve tubes change phloem translocation. J. Exp. Bot. 45, 463–469.
Fromm, J., Lautner, S., 2007. Electrical signals and their physiological significance in plants. Plant Cell Environ. 30, 249–257.
Fromm, J., Spanswick, R., 1993. Characteristics of action potentials in willow (*Salix viminalis* L.). J. Exp. Bot. 44, 1119–1125.
Fromm, J., Hajirezaei, M., Wilke, I., 1995. The biochemical response of electrical signalling in the reproductive system of hibiscus plants. Plant Physiol. 109, 375–384.
Garkusha, I.V., Petrov, V.A., Vasiliev, V.A., Romanovsky, Yu.M., 2002. Propagating of bioelectric potentials in green plants'conducting system. Mathematical modeling and experiment. Proc. SPIE 4707, 384–394.
Gradmann, D., 1976. "Metabolic" action potentials in *Acetabularia*. J. Membrane Biol. 29, 23–45.
Gradmann, D., 2001a. Impact of apoplast volume on ionic relations in plant cells. J. Membrane Biol. 184, 61–69.
Gradmann, D., 2001b. Models for oscillations in plants. Aust. J. Plant Physiol. 28, 577–590.
Gradmann, D., Hoffstadt, J., 1998. Electrocoupling of ion transporters in plants: interaction with internal ion concentrations. J. Membrane Biol. 166, 51–59.
Gradmann, D., Blatt, M.R., Thiel, G., 1993. Electrocoupling of ion transporters in plants. J. Membrane Biol. 136, 327–332.
Grams, T.E.E., Koziolek, C., Lautner, S., Matyssek, R., Fromm, J., 2007. Distinct roles of electric and hydraulic signals on the reaction of leaf gas exchange upon re-irrigation in *Zea mays* L. Plant Cell Environ. 30, 79–85.
Grams, T.E.E., Lautner, S., Felle, H.H., Matyssek, R., Fromm, J., 2009. Heat-induced electrical signals affect cytoplasmic and apoplastic pH as well as photosynthesis during propagation through the maize leaf. Plant Cell Environ. 32, 319–326.
Hansen, U.-P., Gradmann, D., Sanders, D., Slayman, C.L., 1981. Interpretation of current–voltage relationships for active ion transport systems: I. Steady-state reaction-kinetic analysis of class-I mechanisms. J. Membrane Biol. 63, 165–190.
Hodick, D., Sievers, A., 1988. The action potential of *Dionaea muscipula* Ellis. Planta 174, 8–18.
Holdaway-Clarke, T.L., Walker, N.A., Hepler, P.K., Overall, R.L., 2000. Physiological elevations in cytoplasmic free calcium by cold or ion injection result in transient closure in higher plant plasmodesmata. Planta 210, 329–335.
Iijima, T., Sibaoka, T., 1985. Membrane potentials in excitable cells of *Aldrovanda vesiculosa* trap-lobes. Plant Cell Physiol. 26, 1–13.
Kinoshita, T., Nishimura, M., Shimazaki, K., 1995. Cytosolic concentration of Ca^{2+} regulates the plasma membrane H^+-ATPase in guard cells of *Fava bean*. Plant Cell 7, 1333–1342.
Koziolek, C., Grams, T.E.E., Schreiber, U., Matyssek, R., Fromm, J., 2003. Transient knockout of photosynthesis mediated by electrical signals. New Phytol. 161, 715–722.

Krol, E., Dziubinska, H., Trebacz, K., 2003. Low-temperature induced transmembrane potential changes in the liverwort *Conocephalum conicum*. Plant Cell Physiol. 44, 527–533.

Krol, E., Dziubinska, H., Trebacz, K., 2004. Low-temperature-induced transmembrane potential changes in mesophyll cells of *Arabidopsis thaliana*, *Helianthus annuus* and *Vicia faba*. Physiol. Plant 120, 265–270.

Krupenina, N.A., Bulychev, A.A., 2007. Action potential in a plant cell lowers the light requirement for non-photochemical energy-dependent quenching of chlorophyll fluorescence. Biochim. Biophys. Acta 1767, 781–788.

Lewis, B.D., Karlin-Neumann, G., Davis, R.W., Spalding, E.P., 1997. Ca^{2+}-activated anion channels and membrane depolarizations induced by blue light and cold in *Arabidopsis* seedlings. Plant Physiol. 114, 1324–1327.

Macpherson, J.V., Unwin, P.R., 1997. Determination of the diffusion coefficient of hydrogen in aqueous solution using single and double potential step chronoamperometry at a disk ultramicroelectrode. Anal. Chem. 69, 2063–2069.

Michelet, B., Boutry, M., 1996. The plasma membrane H^+-ATPase. A highly regulated enzyme with multiple physiological functions. Plant Physiol. 108, 1–6.

Mummert, H., Gradmann, D., 1991. Action potentials in *Acetabularia:* measurement and simulation of voltage-gated fluxes. J. Membrane Biol. 124, 265–273.

Opritov, V.A., Retivin, V.G., 1982. On the mechanism of propagating excitation in higher plants. Fiziol. Rast 29, 915–924.

Opritov, V.A., Pyatygin, S.S., Retivin, V.G., 1991. Biolectrogenesis in higher plants. Nauka, Moskow [in Russian].

Opritov, V.A., Pyatygin, S.S., Vodeneev, V.A., 2002. Direct coupling of action potential generation in cells of a higher plant (*Cucurbita pepo*) with the operation of an electrogenic pump. Russ. J. Plant. Physiol. 49, 142–147.

Opritov, V.A., Lobov, S.A., Pyatygin, S.S., Mysyagin, S.A., 2005. Analysis of possible involvement of local bioelectric responses in chilling perception by higher plants exemplified by *Cucurbita pepo*. Russ. J. Plant Physiol. 52, 801–808.

Pietruszka, M., Stolarek, J., Pazurkiewicz-Kocot, K., 1997. Time evolution of the action potential in plant cells. J. Biol. Phys. 23, 219–232.

Pyatygin, S.S., 2008. Are there different velocity types of action potentials in higher plants? Biophysics 53, 81–86.

Pyatygin, S.S., Opritov, V.A., Abramova, N.N., Vodeneev, V.A., 1999. Primary bioelectric response of higher plant cells to the combined action of stress factors. Russ. J. Plant. Physiol. 46, 530–536.

Pyatygin, S.S., Opritov, V.A., Polovinkin, A.V., Vodeneev, V.A., 1999. Mechanism of generation of action potential in higher plants. Dokl. Biophys. 364 – 366, 42–45.

Pyatygin, S.S., Opritov, V.A., Vodeneev, V.A., 2008. Signaling role of action potential in higher plants. Russ. J. Plant. Physiol. 55, 312–319.

Qu, Z., Garfinkel, A., 1999. An advanced algorithm for solving partial differential equation in cardiac conduction. IEEE Trans. Biomed. Eng. 46, 1166–1168.

Ryser, C., Wang, J., Mimietz, S., Zimmermann, U., 1999. Determination of the individual electrical and transport properties of the plasmalemma and the tonoplast of the giant marine alga *Ventricaria ventricosa* by means of the integrated perfusion/charge-pulse technique: evidence for a multifolded tonoplast. J. Membrane Biol. 168, 183–197.

Samejima, M., Sibaoka, T., 1982. Identification of the excitable cells in the petiole of *Mimosa pudica* by intracellular injection of procion yellow. Plant Cell Physiol. 24, 33–39.

Samson, E., Marchand, J., Snyder, K.A., 2003. Calculation of ionic diffusion coefficients on the basis of migration test results. Mater. Struct./Mater. Construct. 36, 156–165.

Shabala, S., Shabala, L., Gradmann, D., Chen, Z., Newman, I., Mancuso, S., 2006. Oscillations in plant membrane transport: model predictions, experimental validation, and physiological implications. J. Exp. Bot. 57, 171–184.

Shajahan, T.K., Nayak, A.R., Pandit, R., 2009. Spiral-wave turbulence and its control in the presence of inhomogeneities in four mathematical models of cardiac tissue. PLoS ONE 5, e4738.

Sibaoka, T., 1962. Excitable cells in mimosa. Science 137, 226.

Sibaoka, T., 1991. Rapid plant movements triggered by action potentials. Bot. Mag. Tokyo 104, 73–95.

Spanswick, R.M., 1972. Electrical coupling between cells of higher plants: a direct demonstration of intercellular communication. Planta (Berl.) 102, 215–227.

Spanswick, R.M., 2006. Electrogenic pumps. In: Volkov, A.G. (Ed.), Plant Electrophysiology. Theory and Methods, Springer, Berlin-Heidelberg, pp. 221–246.

Stankovic, B., Davies, E., 1996. Both action potentials and variation potentials induce proteinase inhibitor gene expression in tomato. FEBS Lett. 390, 275–279.

Stankovic, B., Witters, D.L., Zawadzki, T., Davies, E., 1998. Action potentials and variation potentials in sunflower: an analysis of their relationships and distinguishing characteristics. Physiol. Plant 105, 51–58.

Sukhov, V.S., Vodeneev, V.A., 2005. Mathematical model of action potential in higher plant. In: Riznichenko, G.Y. (Ed.), Mathematics, Computing, Education. "Regular and chaotic dynamics", Moskow-Izhevsk, , pp. 267 – 278 (in Russian).

Sukhov, V.S., Vodeneev, V.A., 2009. A mathematical model of action potential in cells of vascular plants. J. Membrane Biol. 232, 59–67.

Sukhov, V.S., Nerush, V.N., Vodeneev, V.A., 2011. An investigation of an action potential propagation in vascular plant using FitzHugh – Nagumo model. Comput. Res. Model. 3, 77–84 (in Russian).

Ten Tusscher, K.H.W.J., Panfilov, A.V., 2006. Cell model for efficient simulation of wave propagation in human ventricular tissue under normal and pathological conditions. Phys. Med. Biol. 51, 6141–6156.

Ten Tusscher, K.H.W.J., Bernus, O., Hren, R., Panfilov, A.V., 2006. Comparison of electrophysiological models for human ventricular cells and tissues. Prog. Biophys. Mol. Biol. 90, 326–345.

Thiel, G., MacRobbie, E.A.C., Blatt, M.R., 1992. Membrane transport in stomatai guard cells: the importance of voltage control. J. Membrane Biol. 126, 1–18.

Trebacz, K., Dziubinska, H., Krol, E., 2006. Electrical signals in long-distance communication in plants. In: Baluska, F., Mancuso, S., Volkmann, D. (Eds.), Communication in Plants. Neuronal Aspects of Plant Life, Springer, Berlin-Heidelberg, pp. 277–290.

Trewaves, A., 1999. Le Calcium, C'est la via: calcium makes waves. Plant Physiol. 121, 1–6.

Tyerman, S.D., Beilby, M., Whittington, J., Juswono, U., Neyman, L., Shabala, S., 2001. Oscillations in proton transport revealed from simultaneous measurements of net current and net proton fluxes from isolated root protopasts: MIFE meets patch-clamp. Aust. J. Plant Physiol. 28, 591–604.

Vodeneev, V.A., Opritov, V.A., Pyatygin, S.S., 2006. Reversible changes of extracellular pH during action potential generation in a higher plant *Cucurbita pepo*. Russ. J. Plant. Physiol. 53, 481–487.

Vodeneev, V.A., Pyatygin, S.S., Opritov, V.A., 2007. Reversible change of extracellular pH at the generation of mechano-induced electrical reaction in a stem of *Cucurbita pepo*. Plant Signal. Behav. 2, 267–268.

Volkov, A.G., 2000. Green plants: electrochemical interfaces. J. Electroanal. Chem. 483, 150–156.

Volkov, A.G., Haack, R.A., 1995. Insect induced bioelectrochemical signals in potato plants. Bioelectrochem. Bioenerg. 35, 55–60.

Wacke, M., Thiel, G., 2001. Electrically triggered all-or-none Ca^{2+}-liberation during action potential in the giant alga *Chara*. J. Gen. Physiol. 118, 11–22.

Wohlfart, B., Ohlen, G., 1999. Properties of spiral waves in a piece of isotropic myocardium. Clin. Physiol. 19, 11–21.

Zawadzki, T., Davies, E., Dziubinska, H., Trebacz, K., 1991. Characteristics of action potentials in *Helianthus annus*. Physiol. Plant 83, 601–604.

Zawadzki, T., Dziubinska, H., Davies, E., 1995. Characteristics of action potentials generated spontaneously in *Helianthus annus*. Physiol. Plant 93, 291–297.